

The Energy Sources of Superluminous Supernovae

Shan-Qin Wang^{1,2,3}, Ling-Jun Wang⁴, Zi-Gao Dai^{1,3}

¹ School of Astronomy and Space Science, Nanjing University, Nanjing 210093, China; dzg@nju.edu.cn

² Guangxi Key Laboratory for Relativistic Astrophysics, School of Physical Science and Technology, Guangxi University, Nanning 530004, China; shanqinwang@gxu.edu.cn

³ Key Laboratory of Modern Astronomy and Astrophysics (Nanjing University), Ministry of Education, China

⁴ Astroparticle Physics, Institute of High Energy Physics, Chinese Academy of Sciences, Beijing 100049, China

Abstract Supernovae (SNe) are the most brilliant optical stellar-class explosions. Over the past two decades, several optical transient survey projects discovered more than ~ 100 so-called superluminous supernovae (SLSNe) whose peak luminosities and radiated energy are $\gtrsim 7 \times 10^{43} \text{ erg s}^{-1}$ and $\gtrsim 10^{51} \text{ erg}$, at least an order of magnitude larger than that of normal SNe. According to their optical spectra features, SLSNe have been split into two broad categories of type I that are hydrogen-deficient and type II that are hydrogen-rich. Investigating and determining the energy sources of SLSNe would be of outstanding importance for understanding the stellar evolution and explosion mechanisms. The energy sources of SLSNe can be determined by analyzing their light curves (LCs) and spectra. The most prevailing models accounting for the SLSN LCs are the ^{56}Ni cascade decay model, the magnetar spin-down model, the ejecta-CSM interaction model, and the jet-ejecta interaction model. In this *review*, we present several energy-source models and their different combinations.

Key words: stars: magnetars – supernovae: general

1 INTRODUCTION

Supernovae (SNe) are believed to be violent explosions of massive stars or white dwarfs. The peak luminosities and radiated energies of normal SNe are $\sim 10^{42} - 10^{43} \text{ erg s}^{-1}$ and $\sim 10^{49} \text{ erg}$, respectively. According to their optical spectra around the peaks, SNe can be divided into type I whose spectra lack hydrogen lines and type II whose spectra show hydrogen lines (Minkowski, 1941; Filippenko, 1997).

Over the past two decades, several sky-survey projects for optical transients have discovered about 100 ultra-luminous SNe (e.g., Quimby et al. 2011; Chomiuk et al. 2011; Nicholl et al. 2014; Quimby 2014; De Cia et al. 2018; Lunnan et al. 2018) whose peak luminosities and radiated energies are $\gtrsim 7 \times 10^{43} \text{ erg s}^{-1}$ (absolute magnitudes in any band must be $\lesssim -21 \text{ mag}$ (Gal-Yam, 2012)¹) and $\gtrsim 10^{51} \text{ erg}$, respectively. These highly luminous SNe are coined “superluminous supernovae (SLSNe)” (for reviews focusing on observations, see Gal-Yam 2012, 2018).

Like normal SNe, SLSNe can be divided into types I (hydrogen-poor) and II (hydrogen-rich). To date, almost all type I SLSNe are helium-deficient and are therefore type Ic. The spectra of most of

¹ Gal-Yam (2018) suggest that the threshold can be set to be $M_g < -19.8 \text{ mag}$.

type I SLSNe resemble those of the SNe Ic (Pastorello et al., 2010; Gal-Yam, 2012; Inserra et al., 2013; Nicholl et al., 2016b), especially those of SNe Ic-BL (Liu & Modjaz, 2017). Most SLSNe II are SLSNe IIn whose spectra have narrow- and intermediate-width $H\alpha$ emission lines (Smith et al., 2007), similar to those of SNe IIn (Schlegel et al., 1990, 1996; Filippenko, 1997). The prototype SLSN IIn is SN 2006gy (Smith et al., 2007). So far, only two confirmed SLSNe are of type IIL: SN 2008es (Gezari et al., 2009; Miller et al., 2009) and SN 2013hx (Inserra et al., 2018). The similarity between SLSNe Ic/IIn and SNe Ic-BL/IIn indicates that SLSNe are likely originated from the explosions of massive stars since SNe Ic-BL/IIn are believed to be produced by the explosions of massive stars.

According to the characteristics of their light curves (LCs), most SLSNe I can be divided into two groups: fast-evolving (Quimby et al., 2011; Inserra et al., 2013; Nicholl et al., 2014) and slow-evolving ones (Gal-Yam et al., 2009; Nicholl et al., 2013, 2016a; Inserra et al., 2017). However, the LC behaviors of SLSNe are rather heterogeneous and some SLSNe can be classified into neither fast-evolving nor slow-evolving, (e.g., Gaia16apd Nicholl et al. 2017a; Kangas et al. 2017; Yan et al. 2017), being transitional objects between these two types. The LCs of some SLSNe I show double-peaked structure (Nicholl et al., 2015a; Nicholl & Smartt, 2016; Smith et al., 2016; Vreeswijk et al., 2017). While the LCs of SLSNe II are more complicated than that of SLSNe I, all of them do not show double-peaked structure.

SLSNe tend to explode in low-metallicity dwarf galaxies (Young et al., 2010; Neill et al., 2011; Chen et al., 2013; Lunnan et al., 2014, 2015) and the star formation rates (SFRs) of the host galaxies of SLSNe are usually high. To date, only very few SLSNe were found in giant, metal-rich galaxies, e.g., SN 2006gy (Smith et al., 2007) and SN 2017egm (Nicholl et al., 2017b; Bose et al., 2018).

Determining the energy sources powering the LCs of SLSNe is of outstanding importance for understanding the stellar evolution and explosion mechanisms. We can conclude that the LCs of most ordinary SNe must be powered by ^{56}Ni cascade decay (e.g., Colgate & McKee 1969; Colgate et al. 1980; Arnett 1982; Cappellaro et al. 1997; Valenti et al. 2008; Chatzopoulos et al. 2012; Piro & Nakar 2013), and/or ionized hydrogen recombination (e.g., Popov 1993; Dessart & Hillier 2005; Kasen & Woosley 2009), and a minor of SNe might be powered by ejecta–circumstellar medium (CSM) interaction (e.g., Chevalier 1982; Chevalier & Fransson 1994; Chugai & Danziger 1994; Chugai 2009), or neutron-star/magnetar spin-down (Ostriker & Gunn, 1971; Maeda et al., 2007). Unlike ordinary SNe, the energy sources of SLSNe are still elusive and in debate. To date, the most promising energy-source models accounting for the SLSN observations are pair instability SN model (Barkat et al., 1967; Rakavy & Shaviv, 1967; Heger & Woosley, 2002; Heger et al., 2003) which is essentially the ^{56}Ni cascade decay model but required ^{56}Ni ($(\gtrsim 5M_{\odot})$) are significantly larger than that for powering ordinary SNe ($\lesssim 0.6M_{\odot}$), the magnetar model (Kasen & Bildsten, 2010; Woosley, 2010; Chatzopoulos et al., 2012, 2013b; Inserra et al., 2013; Chen et al., 2015; Wang et al., 2015a, 2016b; Dai et al., 2016), the ejecta–CSM interaction model (Chevalier & Irwin, 2011; Chatzopoulos et al., 2012; Liu et al., 2018), and the fallback (jet-ejecta interaction) model (Dexter & Kasen, 2013). All These models suppose that the released high-energy photons get absorbed and heat the ejecta, eventually becoming UV–optical–NIR emission. In this *Review*, we describe these energy-source models and their combinations and discuss their implications for SLSNe.

2 SINGLE ENERGY-SOURCE MODELS

The energy-source models interpreting the unique peak (for single-peaked LCs) or the second peak (for double-peaked LCs) of SNe (and SLSNe) are mainly the ^{56}Ni model, the magnetar model, the ejecta–CSM interaction model, and the fallback (jet-ejecta interaction) model. In some cases, the combinations of two or three energy sources must be taken into account. In this section, we focus on the single energy-source model based on the semi-analytic descriptions.

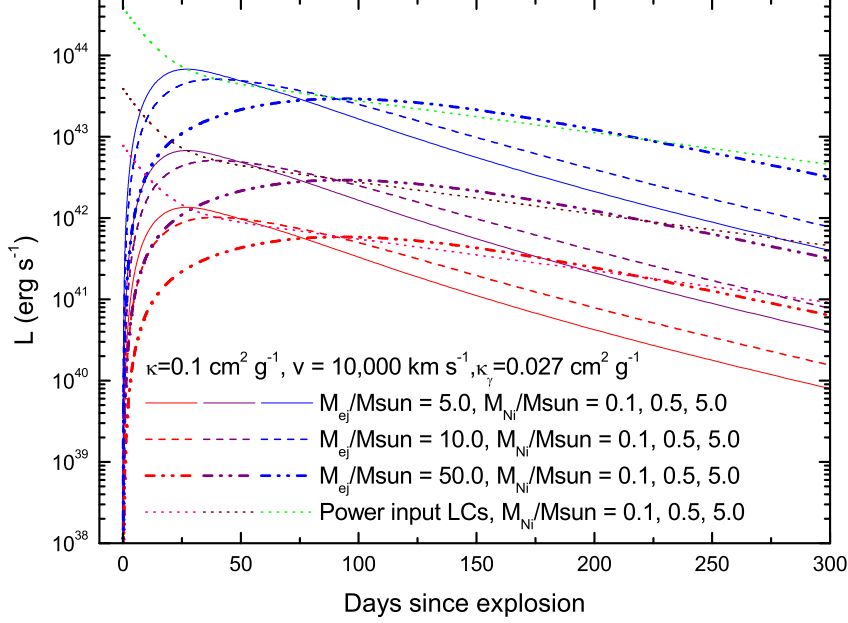


Fig. 1 LCs powered by ^{56}Ni cascade decay. We fix $\kappa = 0.1 \text{ cm}^2 \text{ g}^{-1}$, $v_{\text{sc}} = 10^9 \text{ cm s}^{-1}$. The LCs powered by same amount of ^{56}Ni are presented by same colors.

2.1 The ^{56}Ni Model

When massive stars explode as Fe-core core-collapse SNe (CCSNe, Baade & Zwicky 1934; Janka et al. 2007; Janka 2012), they launch energetic shocks which can heat the stellar mantles to a temperature $\gtrsim 5 \times 10^9 \text{ K}$. Shock-heated silicon shells would synthesize a great amount of radioactive elements, e.g., ^{56}Ni , ^{57}Ni , ^{44}Ti , and ^{22}Na , etc. At early epochs ($\lesssim 500$ days), the power coming from ^{56}Ni is significantly larger than that released by all other elements (Lundqvist et al., 2001; Sollerman et al., 2002). Due to the large distance, many SLSNe and luminous SNe lack late-time photometric observations, the contribution from ^{57}Ni , ^{44}Ti , and ^{22}Na can be therefore neglected in modeling of LCs of these SNe and radioactive-powered model are equal to ^{56}Ni -powered model.

We plot some LCs powered by different amount of ^{56}Ni in Fig. 1. By fixing κ (the optical opacity of the ejecta) = $0.1 \text{ cm}^2 \text{ g}^{-1}$, v_{sc} (the scale velocity of the ejecta) = 10^9 cm s^{-1} , κ_{γ} (the gamma opacity of the ejecta) = $0.027 \text{ cm}^2 \text{ g}^{-1}$, and setting M_{ej} (the mass of the ejecta) = 5, 10, 50 M_{\odot} , M_{Ni} (the mass of ^{56}Ni) = 0.1, 0.5, 5.0 M_{\odot} , we plot 12 LCs, three of which are ^{56}Ni cascade decay input LCs and nine of which are SN LCs powered by ^{56}Ni cascade decay. Adopting this set of parameters, Fig. 1 shows that the ^{56}Ni model can reasonably explain normal SNe, but is difficult to be used to explain the LCs of SLSNe ($L_{\text{peak}} \gtrsim 7 \times 10^{43} \text{ erg s}^{-1}$) since the ratio of M_{Ni} to M_{ej} are unreasonably large (5.0/5.0=1, 5.0/10.0=0.5 for the two most luminous LCs).

Being more luminous than ordinary SNe by a factor of $\sim 10 - 100$ or more, the required ^{56}Ni are usually (significantly) larger than $\sim 5M_{\odot}$ which cannot be synthesized by CCSNe since the ^{56}Ni yields of CCSNe cannot exceed $\sim 4M_{\odot}$ (Umeda & Nomoto 2008). Supposing that the LCs of SLSNe are

powered by ^{56}Ni , the unique method to solve this problem is supposing that the explosions are the so-called “pair instability SNe” (PISNe) (Barkat et al., 1967; Rakavy & Shaviv, 1967; Heger & Woosley, 2002; Heger et al., 2003). For example, Gal-Yam et al. (2009) suggested that SN 2007bi is a PISN; Cooke et al. (2012) studied two high-redshift SLSNe and concluded that these two SLSNe might be PISNe.

2.1.1 Fast-Evolving SLSNe I

Fast-evolving SLSNe I which constitute a major fraction of SLSNe I cannot be explained by the ^{56}Ni models since the decline rates of most of them are larger than that of LCs produced by the ^{56}Ni model (e.g., Quimby et al. 2011). In other words, the ^{56}Ni masses inferred from the peak luminosities are significantly larger than that inferred from the late-time light curves (e.g., De Cia et al. 2018).

Moreover, for all fast-evolving SLSNe I, high peak luminosities require huge amount of ^{56}Ni while the narrow LCs indicate that the masses of the ejecta are relatively small. Inserra et al. (2013) and Nicholl et al. (2014) modeled some fast-evolving SLSNe I and found that the amount of ^{56}Ni are 5 – 30 M_{\odot} and the masses of the ejecta are between several M_{\odot} to 30 M_{\odot} , therefore the ratio of required masses of ^{56}Ni to the ejecta masses are usually $\gtrsim 50\%$ or even 100%, significantly larger than the upper limit ($\sim 20\%$, Umeda & Nomoto 2008) of the ratio of the ^{56}Ni mass to the ejecta mass.

These studies demonstrated that the ^{56}Ni models (including CCSN model and PISN model) cannot account for fast-evolving SLSNe I.

2.1.2 Slow-Evolving SLSNe I

Only very few SLSNe I having slow-evolving post-maximum LCs mimicking that of SNe powered by radioactive elements (mainly ^{56}Ni) might be PISNe (Gal-Yam et al., 2009; Cooke et al., 2012) whose ^{56}Ni masses and ejecta masses can be $\gtrsim 5M_{\odot}$ and 100 – 110 M_{\odot} , respectively. Gal-Yam (2012) proposed that they belong to a distinct class whose energy source is radioactive elements and named this class “SLSNe R”.

However, Dessart et al. (2012) argued that SN 2007bi was not a PISN since its spectra are not consistent with that reproduced by PISN models. Alternatively, Dessart et al. (2012) suggested that SN 2007bi was powered by a magnetar. Moreover, Inserra et al. (2017) found that the declined rates of the LCs at $t - t_{\text{peak}} \gtrsim 150$ days of four slow-evolving SLSNe I (SN 2007bi, PTF12dam, SN 2015bn, and LSQ14an) are inconsistent with that of LCs reproduced by ^{56}Co decay, indicating that they cannot be explained by PISN model since the ejecta masses of PISNe are very large so that the decline rates of their LCs must be consistent with that of ^{56}Co decay rate at $t - t_{\text{peak}} \lesssim 500$ days.

2.1.3 SLSNe II

Studies for some type II SLSNe, e.g., SN 2006gy (Agnoletto et al., 2009) and CSS121015 (Inserra et al., 2013), also demonstrated that the LCs of SLSNe II cannot be explained by both normal ^{56}Ni model and the PISN model.

In summary, to date, only a small fraction SLSNe might be powered by the decay of ^{56}Ni that were synthesized by PISNe, most SLSNe cannot be explained by ^{56}Ni and must be accounted for by other models.

2.2 The Magnetar Model

CCSN explosions may leave behind fast-rotating neutron stars whose initial rotational periods (P_0) are several milliseconds to several seconds. Based on the observations for some SN remnants (SNRs), Ostriker & Gunn (1971) proposed that neutron stars with magnetic field strength $B \sim 10^{12}$ G can play a key role in energizing both SNe and SNRs by injecting their rotational energy to the ejecta or shells.

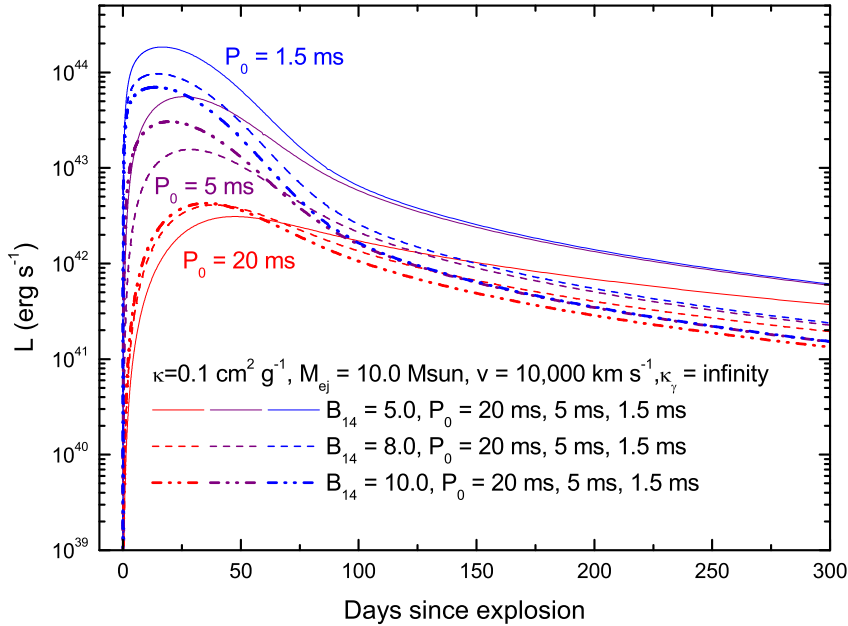


Fig. 2 LCs powered by magnetar model. We fix $\kappa = 0.1 \text{ cm}^2 \text{ g}^{-1}$, $M_{\text{ej}} = 10M_{\odot}$, $v_{\text{sc}} = 10^9 \text{ cm s}^{-1}$. The LCs powered by magnetars with same initial rotational periods are presented by same colors.

The same model has been applied for modeling GRB prompt emission (Usov, 1992; Metzger et al., 2007; Bucciantini et al., 2008; Metzger et al., 2011) and GRB afterglows (e.g., Dai & Lu 1998a,b; Zhang & Mészáros 2001; Dai 2004; Dai & Liu 2012). In these models, the neutron stars are highly magnetized, $B \sim 10^{14-15} \text{ G}$, and are called “magnetars”.

The magnetar spinning-down model had also been introduced to study SNe. To account for the LC of SN 2005bf which is not very luminous but cannot be explained by ^{56}Ni model, Maeda et al. (2007) suggested that the energy source powering it is a newly-born magnetar and the initial spin period is $\sim 10 \text{ ms}$. Woosley (2010) and Kasen & Bildsten (2010) suggested that LCs of SLSNe can be powered by spinning-down magnetars whose initial spin periods and magnetic strength are $\sim 1 - 5 \text{ ms}$ and $\sim 10^{14-15} \text{ G}$, respectively.²

The shapes and peak luminosities of the LCs powered by magnetars depend sensitively on the values of κ , M_{ej} , v_{sc} , B , and P_0 . Supposing $\kappa = 0.1 \text{ cm}^2 \text{ g}^{-1}$, $v_{\text{sc}} = 10^9 \text{ cm s}^{-1}$, $M_{\text{ej}} = 10M_{\odot}$, $\kappa_{\gamma} = \text{infinity}$ (full trapping), and setting $B_{14} = B/10^{14}\text{G} = 5, 8, 10$, $P_0 = 20, 5, 1.5 \text{ ms}$, we plot 9 LCs powered by magnetars in Figure 2. Adopting this set of parameters, Figure 2 shows that the magnetar model can reasonably explain normal SNe, luminous SNe, as well as SLSNe. If we fix the values of B and P_0 and vary the values of κ , M_{ej} , and v_{sc} , we can also get different LCs. Like the ^{56}Ni model, larger M_{ej} and κ or lower v_{sc} would result in dimmer peaks and broad LCs.

² Wang et al. (2016a, 2017a,c) and Chen et al. 2017 demonstrated that the LCs of some broad-lined SNe Ic might be powered by millisecond magnetars if the magnetic strength of these putative magnetars are a few 10^{16} G .

Inserra et al. (2013), Nicholl et al. (2013), and Nicholl et al. (2014) used the magnetar model with full trapping of high energy photons (gamma rays and X-rays) to fit the LCs of some SLSNe I and found that the LCs reproduced by this model are in good agreement with the observational data. As mentioned above, the model adopted by these groups was derived on the assumption of full-trapping of the gamma-ray and X-ray emission. When the hard emission was mainly the X-ray emission, this assumption is valid and the LCs reproduced by this model can be in good/excellent agreement with observations. If the high-energy emission was dominated by the gamma-ray emission, a fraction of hard emission would leak from the ejecta before being soften to be UV–optical–IR photons. Therefore, some LCs reproduced by the model with the assumption have the tails brighter than the observation (Nicholl et al., 2014; Chen et al., 2015).

To solve this problem, Wang et al. (2015a) incorporated the leakage effect into the original magnetar-powered model. If the magnetar emission is dominated by gamma-ray ($E_\gamma \gtrsim 10^6$ eV), $\kappa_\gamma \simeq 0.01 - 0.2 \text{ cm}^2 \text{ g}^{-1}$; if the emission is dominated by X-ray ($10^2 \text{ eV} \lesssim E_X \lesssim 10^6 \text{ eV}$), $\kappa_X \simeq 0.2 - 10^4 \text{ cm}^2 \text{ g}^{-1}$, (see Fig. 8 of Kotera et al. 2013). By analyzing the late-time LC of PTF12dam, Chen et al. (2015) also found the magnetar model with full trapping cannot fit the late-time LC of PTF12dam and introduced a similar trapping factor. Using this revised magnetar-powered model, the SLSNe whose LC tails cannot be fitted by the magnetar model with full trapping were well explained, see, e.g., Figure 3.

Although Woosley (2010) and Kasen & Bildsten (2010) had demonstrated the acceleration effect is rather notable, the models based on Arnett (1982) all neglect acceleration of the SN ejecta caused by the magnetar wind. Besides, the photospheric recession effect is also omitted in these models. Wang et al. (2016b) proposed a new semi-analytic magnetar-powered model that has taken these two effects into account. In this new magnetar-powered model, the photospheric velocity of a SLSN is smaller than the scale velocity v_{sc} and its evolution must be fit. Moreover, the scale velocity itself is a running quantity and is not a parameter or a measurable quantity. Instead, the initial scale velocity v_{sc0} is a free parameter.

Using this model, Liu et al. (2017) fitted the data of 19 SLSNe I and found that the LCs, temperature evolution, and photometric velocity evolution reproduced by this model are in good agreement with the observations and $\sim 19\text{--}97\%$ of initial rotational energy of the magnetars was converted to the kinetic energy of the ejecta. Moreover, they found that the initial kinetic energies of most of these SLSNe are smaller than $\sim 2 \times 10^{51}$ erg which is the upper limit of the kinetic energies that can be provided by neutrino-powered mechanism (Ugliano et al., 2012; Janka, 2012; Sukhbold et al., 2016).

Soker & Gilkis (2017) investigated 38 SLSNe I discovered by the Pan-STARRS1 medium deep survey (PS1 MDS, Lunnan et al. 2018) and suggested that the SLSNe which are supposed to be powered by magnetars should be firstly powered by jets launched from the surfaces of the magnetars. Further investigations for the magnetar model are needed.

For a SLSN that can be explained by a magnetar, the contribution from ^{56}Ni can be neglected since a SLSN leaving a magnetar is a CCSN whose ^{56}Ni yield is usually rather low, $\lesssim 0.2M_\odot$, and the luminosity from this amount of ^{56}Ni is significantly smaller than that of a SLSN (Inserra et al., 2013).

2.3 The Ejecta-CSM Interaction Model

Before the explosions, the progenitors of SNe are surrounded by the circumstellar winds or material shells ejected from the progenitors just prior to the SN explosions. After the explosions, the SN ejecta collide with the winds or shells, generating forward shocks and reverse shocks whose dynamics can be described by the self-similar solutions (Chevalier, 1982; Chevalier & Fransson, 1994). In some extreme cases, the “pulsational pair-instability (PPI)” mechanism (Heger et al., 2003; Woosley et al., 2007; Pastorello et al., 2008; Chugai, 2009; Chatzopoulos & Wheeler, 2012) might expel some shells in different epochs, faster shells might catch up and collide the slower shells, also generating forward shocks and reverse shocks. The shock-accelerated electrons emit gamma- and X-ray photons and most of these photons would be soften to UV–optical–IR photons. These processes convert the kinetic energy of the ejecta or the faster shells to the radiative energy of the SNe and might significantly increase the luminosities of some SNe if the density of circumstellar wind or shells is high enough.

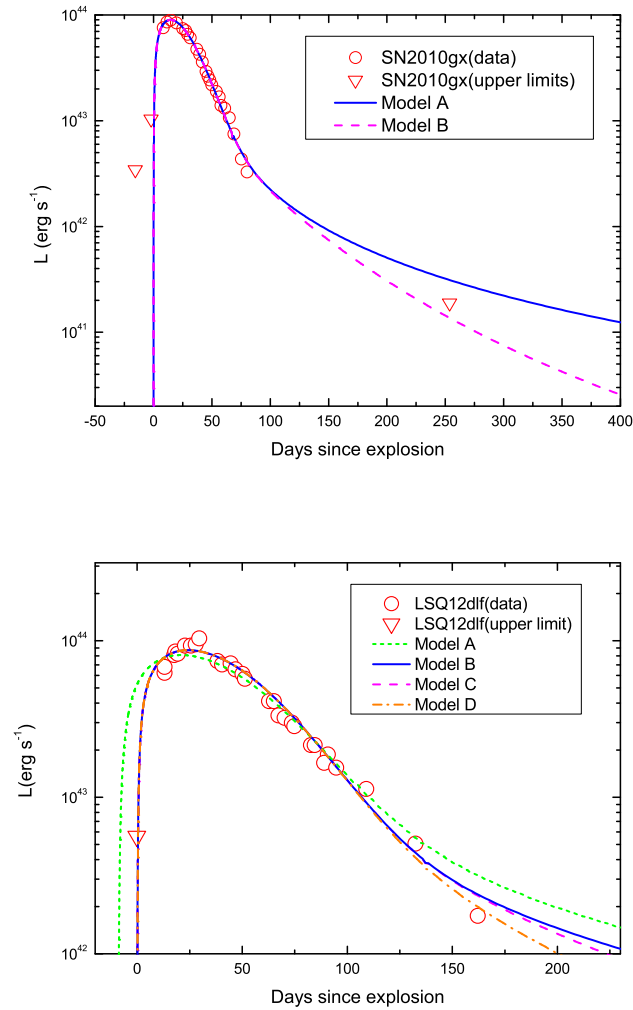


Fig. 3 LCs in the original magnetar-powered model and the revised magnetar-powered model for SN 2010gx, and LSQ12dlf. The solid lines and dashed lines are produced by the magnetar models without and with leakage effect, respectively (Wang et al., 2015a).

The LCs of SLSNe IIn cannot be explained by any model neglecting the contributions from the interaction-induced shocks. In fact, the ejecta-CSM interaction model in which the LCs of these SNe are powered by interaction between the SN ejecta and the hydrogen-rich (and hydrogen-poor) CSM is the most natural model explaining SNe IIn (e.g., Chugai & Danziger 1994; Miller et al. 2010; Zhang et al. 2012), Ibn (e.g., Chugai 2009), as well as SLSNe IIn (e.g., Smith & McCray 2007; Moriya et al. 2013; Nicholl et al. 2014). Since the properties of CSM are very complicated, the LCs of luminous SNe IIn, Ibn, and SLSNe IIn aided by the ejecta-CSM interaction show great complexity (see Smith 2016 and references therein).

Many studies have demonstrated that the LCs of SLSNe I and SLSNe IIL whose spectra are lack of narrow lines indicative of ejecta-CSM interactions or shell-shell interactions can be explained by the magnetar-powered model. Although the absence of the interaction signatures in the spectra of SLSNe I and IIL indicates that the contributions from the interactions can be neglected in explaining these two classes of SLSNe, the possibility that these SLSNe are powered by interactions cannot be excluded since the interaction is not necessary to prompt corresponding signs (e.g., narrow and intermediate-width H α emission lines).

Ginzburg & Balberg (2012) used the interaction model to fit the LCs of SN 2010gx (type I) and SN 2006gy (type IIn). Nicholl et al. (2014) also used this semi-analytic model to fit some SLSNe I since the late-time LCs reproduced by the magnetar-powered model neglecting late-time leakage are inconsistent with the observations. Tolstov et al. (2016) argue that PTF12dam (SLSN I) can be powered by the shell-shell collision.

Recently, Liu et al. (2018) constructed an ejecta–CSM interaction model involving multiple interactions between the ejecta and different shells/winds and fit the LCs of iPTF13edcc and iPTF15esb, see Fig 4.

2.4 The Fallback (jet-ejecta Interaction) Model

The collapsar model (Woosley, 1993; MacFadyen & Woosley, 1999) for gamma ray bursts (GRBs) proposes that a black hole-disk system can launch a relativistic jet which can punch a hole in the mantle of a stripped progenitor and produce gamma ray emission. In this model, the Fe core collapses to a black hole and the inner mantle material with high angular momentum falls back and forms an accretion disk.

If the jet cannot breakout and is trapped by the stellar mantle, the energy carried by the jet will be deposited and thermalized to black-body emission. Dexter & Kasen (2013) studied this possibility and found that this “failed” jet could significantly change the optical LC powered by the explosion. This model is a jet-ejecta interaction model and can be used to explain SN LCs with different peak luminosities and durations. Wang et al. (2018) explained the unusual type II-P supernova iPTF14hls which is not a SLSN as episodic fallback accretion onto a neutron star. If the deposited energy is large, this model can power a peak luminosity $\gtrsim 10^{44}$ erg s $^{-1}$ and reproduce the LCs of SLSNe I and II. Gao et al. (2016) used a similar model to explain ultra-long GRB 111209A and associated supernova (SN 2011kl).

Moriya et al. (2018) used the fallback model to fit 37 SLSNe I and found that the LCs produced by this model can be consistent with observations. Moreover, they adopted a typical conversion efficiency 10^{-3} and estimated the required total energy of the accretion disk, finding that the inferred mass of the accretion disk is $2 - 700 M_{\odot}$. They concluded that only a fraction of SLSNe I whose rising timescales are relative short ($\lesssim 40$ days) can be explained by this model, or the conversion efficiency must be significantly larger than 10^{-3} . As pointed out by Moriya et al. (2018), it is difficult to distinguish the magnetar model and the fallback model using the LCs produced by these two models.

3 DOUBLE-ENERGY-SOURCE MODELS

3.1 Cooling plus ^{56}Ni /Magnetar/Interaction models

After the SN explosion, an energetic shock must be launched from the center of the SN and the shock-breakout (see Waxman & Katz 2016 and references therein) marked by the UV (for non-relativistic shock breakout) or X-ray/gamma-ray (for relativistic shock breakout) emission would appear and the envelope would be heated to a temperature of millions of Kelvin (K). If the progenitors of SNe/SLSNe have extended envelopes, the cooling emission from shock-heated envelopes would power a LC whose initial luminosity can reach $\gtrsim 10^{42}$ erg s $^{-1}$. The cooling emission from a shock-heated envelope usually peaks at UV–optical band and its duration is usually very short, \sim a few days.

Piro (2015) proposed a concise model that can describe the behavior of the LC and temperature evolution powered by the cooling emission. The free parameters of this model are the optical opacity (κ), mass (M_e) and the initial radius (R_e) of the extended envelope, the mass of the core of the SN

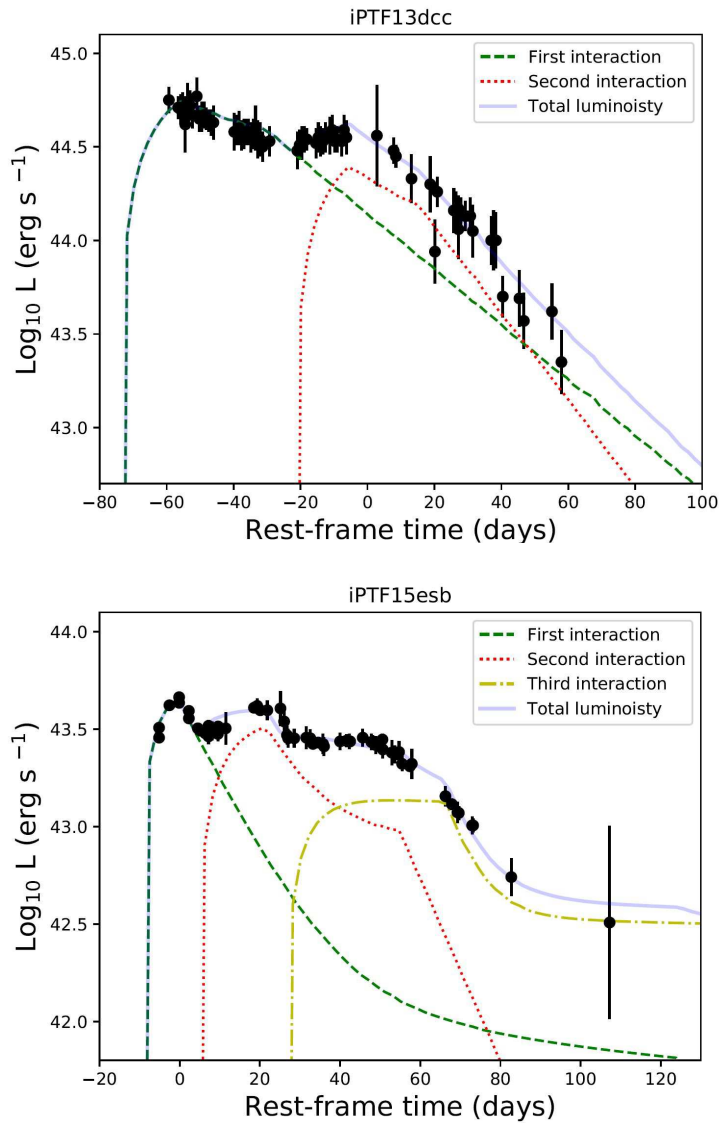


Fig. 4 The bolometric LCs of iPTF13dcc and iPTF15esb and the LCs reproduced by the multiple interaction model (Liu et al., 2018).

(M_c), as well as the kinetic energy of the SN (E_{sn}). The LC plotted in Fig. 5 is yielded by a shock-heated extended envelope model with $\kappa = 0.1 \text{ cm}^2 \text{ g}^{-1}$, $M_e = 0.4 M_{\odot}$, $R_e = 500 R_{\odot}$, $M_c = 5 M_{\odot}$, $E_{\text{sn}} = 6.75 \times 10^{51} \text{ erg}$.

The SLSNe having double-peaked LCs have been observed, e.g., LSQ14bdq (Nicholl et al., 2015a), DES14X3taz (Smith et al., 2016), PTF12dam (Vreeswijk et al., 2017), SN 2006oz (Leloudas et al., 2012; Nicholl & Smartt, 2016), and PS1-10pm (McCrum et al., 2015). Many groups (Nicholl et al., 2015a; Smith et al., 2016; Vreeswijk et al., 2017; Nicholl & Smartt, 2016) suggested that the first peaks

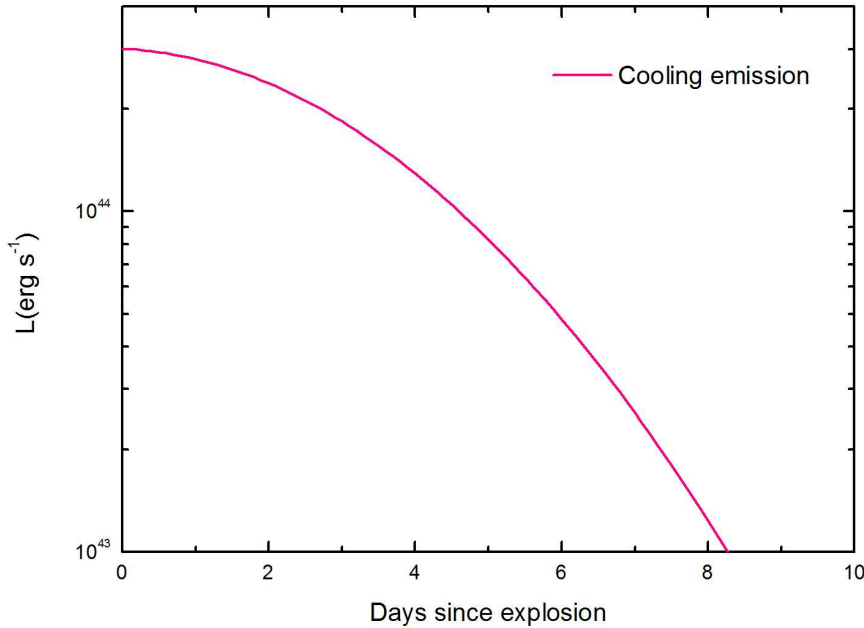


Fig. 5 LC powered by cooling emission from a shock-heated envelope, parameters can be found in the text.

of LCs of these SLSNe were powered by the cooling emission from the shock-heated extended envelopes and the second peaks (main peaks) might be powered by magnetars or ejecta-CSM interactions. In this model, the cooling emission power the first peak and ^{56}Ni synthesized in the shock-heated ejecta or the magnetar left by the explosion or the interaction with the ejecta and the CSM would provide the energy for the second peak and late-time decay. Energy released by other processes would quickly outshine the cooling emission and shape the second LC peak. Fig. 6 shows a LC powered by the cooling emission and a magnetar.

For the SLSNe whose first peaks were missed by observations or have only single peaks, cooling emission can be neglected and their whole LCs might be powered by ^{56}Ni /magnetar/interaction (see subsections 2.1, 2.2, and 2.3) or their combinations (see below).

3.2 The Magnetar plus ^{56}Ni Model

As mentioned above, the contribution from ^{56}Ni cascade decay is significantly smaller than that from other energy sources (magnetar or interaction) and can be neglected in modeling for SLSNe. However, magnetar model and interaction model cannot explain Fe lines (if observed) in the spectra, a moderate amount of ^{56}Ni is needed for explaining the Fe lines related to ^{56}Ni .

Some luminous SNe whose peak magnitudes are between ~ -20 mag and -21 mag (e.g., Deustua et al. 1995; Schmidt et al. 2007; Howell et al. 2006; Sanders et al. 2012; Taddia et al. 2015; Greiner et al. 2015; Roy et al. 2016; Arcavi et al. 2016; Inserra et al. 2018) were also discovered in the

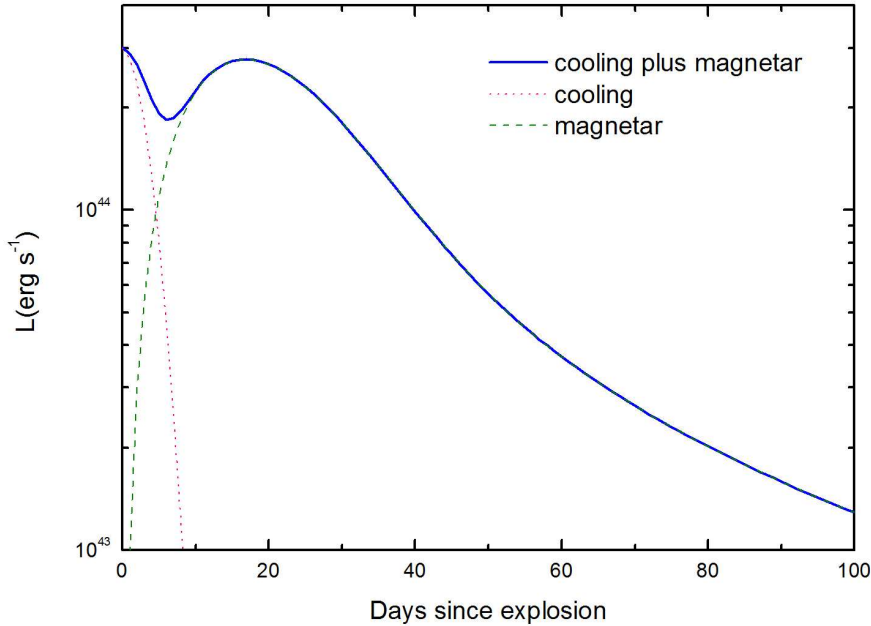


Fig. 6 The LCs reproduced by the cooling model, the magnetar models, and the cooling plus magnetar model. $\kappa = 0.1 \text{ cm}^2 \text{ g}^{-1}$, $M_e = 0.4 M_\odot$, $R_e = 500 R_\odot$, $M_c = 5 M_\odot$, $E_{\text{sn}} = 6.75 \times 10^{51} \text{ erg}$, $v = 1.5 \times 10^9 \text{ cm s}^{-1}$, $B = 3 \times 10^{14} \text{ G}$, $P_0 = 3 \text{ ms}$.

past two decades.³ Wang et al. (2015b) studied three luminous SNe Ic-BL and found that they cannot be explained by ^{56}Ni model.

To solve these two problems, Wang et al. (2015b) proposed that luminous SNe Ic can also be powered by nascent magnetars whose initial rotational periods (P_0) are $\sim 10 \text{ ms}$. Furthermore, Wang et al. (2015b) suggested that the contribution from some amount of ^{56}Ni cannot be omitted since the luminous SNe are not as bright as SLSNe. Therefore, they proposed that these SNe might be powered by magnetars with $P_0 \sim 10 \text{ ms}$ and $\sim 0.1 - 0.2 M_\odot$ of ^{56}Ni . Bersten et al. (2016), Metzger et al. (2015) and Wang et al. (2017d) also employed the double energy sources (magnetar + ^{56}Ni) to fit the most luminous GRB-SN, SN 2011kl.

Recently, Blanchard et al. (2018) studied the multi-band LC and spectra of SN 2017dwh which is a SLSN I exploded at $z \approx 0.13$. Based on the post-peak spectra showing a strong absorption line centered near 3200 \AA which is inferred to be Co II and the late-time spectra which also provides the evidence for the existence of a large mass of Fe-group elements, Blanchard et al. (2018) concluded that this SLSN synthesizes $\lesssim 0.6 M_\odot$ and used magnetar plus ^{56}Ni model to model the multi-band LC and got a rather good result. Blanchard et al. (2018) found that the best-fitting parameter of ^{56}Ni is $0.89_{-0.58}^{+0.52} M_\odot$ (1σ

³ Although some authors (e.g., Bersten et al., 2016; Inserra et al., 2018) regarded these luminous SNe as SLSNe, we still adopt the “ridgeline” ($M_{\text{peak}} = -21 \text{ mag}$) given by Gal-Yam (2012) and suggest that these luminous SNe belong to a class of “gap-filler” events that bridge ordinary SNe and SLSNe (Wang et al., 2015b; Arcavi et al., 2016).

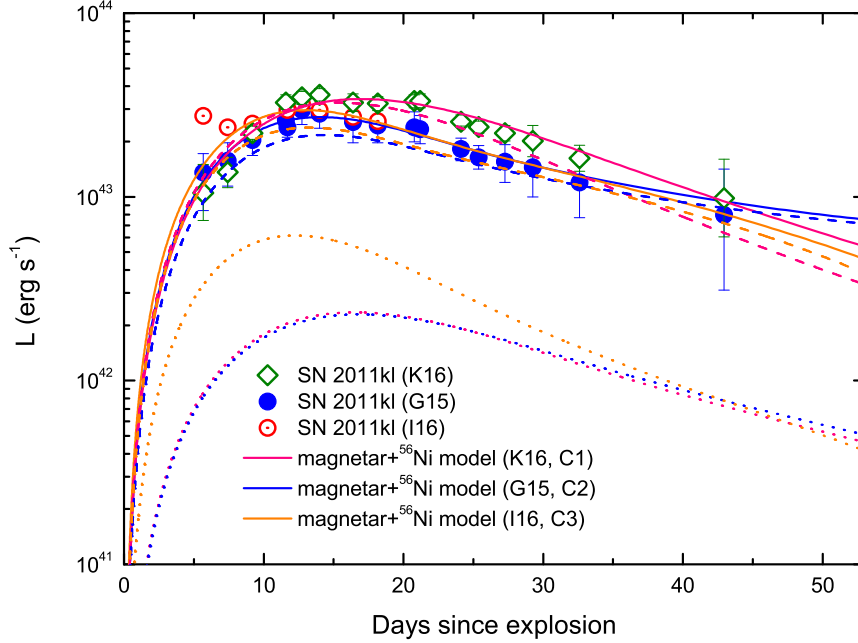


Fig. 7 The magnetar + ^{56}Ni model (solid lines) for the LC of SN 2011kl (Wang et al., 2017d). The dotted lines represent the LCs reproduced by 0.1 (the dimmer LCs) or 0.2 M_{\odot} (the brighter LCs) of ^{56}Ni ; the dashed lines represent the LCs powered by magnetars.

confidence) whose lower limit ($0.31M_{\odot}$) is consistent with the lower limit ($\lesssim 0.6M_{\odot}$) inferred from the spectra.

Based on these studies, we can conclude that some luminous SNe and SLSNe can be explained by the magnetar plus ^{56}Ni model.

3.3 The Interaction plus ^{56}Ni /Magnetar/Fallback Model

To fit the LC of SN 2006gy, Smith & McCray (2007) constructed a double-energy model containing the contributions from shock-heated material and ^{56}Ni cascade decay. This is the ejecta-CSM interaction plus ^{56}Ni model. In this model, the photons coming from shock-heated ejecta and CSM powered the peak-luminosity as well as the early LC while the late-time LC was powered by 8 M_{\odot} of ^{56}Ni . To synthesize this great amount (8 M_{\odot}) of ^{56}Ni , the explosion must be a PISN.

Chatzopoulos et al. (2012) found that the LC of SN 2006gy can be explained by the ejecta-CSM interaction plus 2 M_{\odot} of ^{56}Ni . The inferred ^{56}Ni mass is significantly smaller than that inferred by Smith & McCray (2007). The ejecta mass derived by Chatzopoulos et al. (2012) is 40 M_{\odot} , indicating that, if this result is correct, SN 2006gy is a CCSN rather than a PISN since the final masses (ejecta masses) of PISNe must be $\gtrsim 80M_{\odot}$ (see, e.g., Chatzopoulos et al. 2013a). However, how a CCSN can synthesize 2 M_{\odot} of ^{56}Ni is still a puzzle. Besides, Chatzopoulos et al. 2013b used the interaction plus

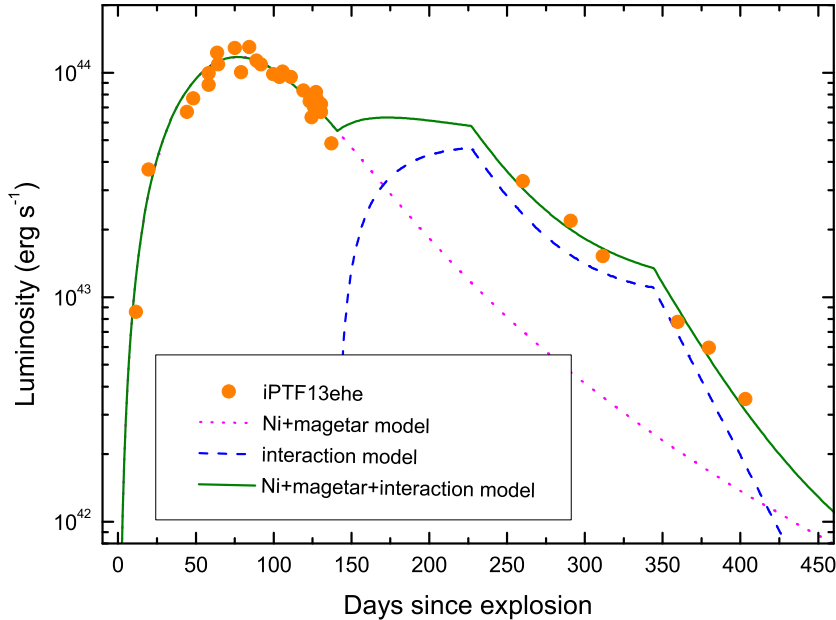


Fig. 8 Modeling LC of iPTF13ehe using the triple-energy model (^{56}Ni + magnetar + interaction) (Wang et al., 2016c).

^{56}Ni model to fit 12 SLSNe (5 SLSNe I and 7 SLSNe II) and got rather good results (they also adopted other models to fit the LCs of these SLSNe).

To fit the LC of the type Ic supernova iPTF16asu whose rise time is as short as four days in rest frame, Wang et al. (2017b) constructed a model including early interaction and late-time energy input from a magnetar. Chen et al. (2018) adopted the interaction plus magnetar model as well as fallback + interaction model to fit the bolometric LC of SLSN 2017ens.

4 TRIPLE-ENERGY-SOURCE MODEL

Yan et al. (2015) studied a type I SLSN, iPTF13ehe, and suggested that its nebula spectra indicate $2.5 M_{\odot}$ of ^{56}Ni . If this SLSN was powered by ^{56}Ni , however, the required ^{56}Ni would be $\gtrsim 13 - 16 M_{\odot}$, significantly larger than the value inferred from the spectral analysis. These facts indicate that the LC of iPTF13ehe cannot be explained by ^{56}Ni model. Wang et al. (2016c) modeled this SLSN using magnetar model and magnetar plus ^{56}Ni model and found both these two models can reproduce the early-time LC of this SLSN.

Since the late-time spectrum shows narrow $\text{H}\alpha$ emission lines indicative of ejecta-CSM interaction and the late-time LC has a brightening feature, Yan et al. (2015) proposed that the ejecta-CSM interaction was triggered when the ejecta collided with the hydrogen-rich CSM shell expelled prior to the explosion and produced late-time brightening as well as $\text{H}\alpha$ emission lines. Wang et al. (2016c) develop a triple energy-source model containing the contributions from ^{56}Ni , magnetar and ejecta-CSM interaction to reproduce the LC of iPTF13ehe; see Fig. 8.

Yan et al. (2015) estimated that $\sim 15\%$ of SLSNe I might have late-time $H\alpha$ emission lines. Obviously, these SLSNe can be explained by double (magnetar plus interaction) or triple energy-source model (^{56}Ni plus magnetar plus interaction).

The models containing cooling emission from the shock-heated envelopes of the SN progenitors and the combinations of ^{56}Ni +magnetar or ^{56}Ni +interaction or magnetar+interaction are also triple energy source models. To account for the LC of SN 2011kl which is a luminous type Ic SN, Wang et al. (2017d) employed the cooling+ ^{56}Ni +magnetar model.

5 DISCUSSION

5.1 The Validity of the Models

Determining the energy sources of the SLSNe is very difficult, but the energy sources should leave their imprints on the SLSN LCs and spectra. For example, if a SLSN is powered by a newly-born magnetar, the magnetar wind would sweep a shell surrounding a bubble. Then the spectra would show velocity plateau Kasen & Bildsten (2010). If a SLSN is powered by the interaction between the ejecta and CSM, there might be some narrow emission lines in their spectra. The narrow $H\alpha$ emission lines are discovered in the spectra of all SNe IIn and SLSNe IIn, then the interaction model is a valid model for explaining SNe IIn and SLSNe IIn. However, as pointed out by Liu & Modjaz (2017), no narrow emission lines are found in the spectra of 32 SLSNe I collected by them, indicting that these SLSNe might not be powered by the interaction. Nevertheless, interactions do not prompt emission lines if the temperature and/or the densities of the CSM is low. Therefore, the interaction model cannot be ruled out.

To test the one-dimensional magnetar model, Liu & Modjaz (2017) analyzed the photospheric velocity evolutions of 13 SLSNe. They found that only two SLSNe I (PTF10hgi and PS1-11ap) show slow velocity-evolution feature that is consistent with the one-dimensional magnetar model and the velocity evolution of the other 11 SLSNe is fast, indicating that the spectra of most SLSNe cannot be explained by one-dimensional magnetar model. However, the two-dimensional magnetar model (Chen et al., 2016) can destroy the shell structure and the spectra might quickly evolve.

By studying the spectra of SN 2015bn, Nicholl et al. (2016b) suggest that the strong and relatively narrow O I $\lambda 7774$ line may indicate the existence of an inner shell swept by a central engine. Furthermore, they argue that the putative central engine might be a magnetar, rather than a black hole. Based on 1000 days of photometric observations for SN 2015bn, Nicholl et al. (2018) find that the light curve at very late epoch is consistent with $L \propto t^{-4}$ which can be yielded by a magnetar spin-down input with inefficient gamma-ray trapping and pointed out that this light-curve feature indicates the existence of a nascent magnetar.

5.2 The Explosion Mechanisms of SLSNe and Luminous SNe

It is believed that the SNe Ia, Iax, and Ia-CSM might have originated from the explosions of white dwarfs and other all sub-classes of normal-luminosity SNe are CCSNe. In contrast, the explosion mechanisms of SLSNe and luminous SNe are still elusive.

It seems that almost all SLSNe II and fast-evolving SLSNe I ever discovered might have been originated from the explosions of CCSNe. However, the explosion mechanisms of slow-evolving SLSNe I are still elusive. Nicholl et al. (2013) modeled the LC of rapid-rising, slow-declining SLSN PTF12dam and analyzed its spectra, concluding that this SLSN cannot be explained by the ^{56}Ni -powered model since the rise time of the LC produced by the ^{56}Ni synthesized by PISNe is larger than that of observed LC. It should be mentioned that Kozyreva & Blinnikov (2015) proposed a PISN model in which ^{56}Ni is strongly mixed into ejecta and the rise time of LCs produced by this PISN model is short enough to fit the observational data. As pointed by Moriya et al. (2017), however, strong ^{56}Ni mixing has not yet been discovered by multidimensional PISN simulations.

5.3 The Progenitors of SLSNe

In the past decades, the progenitors of dozens of SNe have been confirmed directly (see Smartt 2009 and references therein). Unfortunately, none of these SNe is SLSN since all progenitors of SLSNe are too distant ($z \gtrsim 0.1$) to be detected before their explosions.

However, many lines of evidence indicate that the progenitors of SLSNe might be massive stars. The first evidence is that the explosions of white dwarfs cannot produce so bright transients even if the white dwarfs are “super-Chandrasekar” ones. The second evidence is that the spectra of most SLSNe resemble normal-luminosity CCSNe produced by the explosions of massive stars. The third evidence is that most SLSNe are located in star-forming dwarf galaxies.⁴

Almost all SLSNe are located in the low-metallicity dwarf galaxies,⁵ suggesting that the metallicity of the progenitors of SLSNe are rather low. A massive star with low-metallicity has very low mass-loss rate. However, the progenitor of a SLSN I must have lost its hydrogen envelope or even the helium envelope. Therefore, it can be expected that the progenitors of SLSNe I might be in binary systems and the envelopes of the progenitors must be stripped by their companions. This mechanism involving mass transfer has another advantage that the stripping process can spin-up the progenitors and is beneficial for the formations of the millisecond magnetars which might power the LCs of SLSNe.

5.4 SLSN-GRB Connection

A minor fraction of SNe Ic have spectra with very broad absorption troughs which indicate very large photospheric velocities and are named of Broad-lined SNe Ic (SNe Ic-BL) (Woosley & Bloom, 2006). Some SNe Ic-BL associated with long GRBs has been discovered just after the detections of the corresponding GRBs (Galama et al. 1998; Stanek et al. 2003; Hjorth et al. 2003; Gal-Yam et al. 2004; Campana et al. 2006; Mazzali et al. 2006; Berger et al. 2011; Starling et al. 2011; Melandri et al. 2012; Xu et al. 2013; Cano et al. 2014, 2015; D’Elia et al. 2015; Toy et al. 2016; Ashall et al. 2017; Cano et al. 2017a; see Woosley & Bloom 2006; Hjorth & Bloom 2012; Cano et al. 2017b for reviews).

The SNe associated with GRBs are dimmer than SLSNe. To date, the most luminous GRB-SN might be SN 2011kl whose peak bolometric magnitude is $\simeq -20.25 \pm 0.06$ mag (Kann et al., 2016) while the peak bolometric magnitudes of SLSNe are $\lesssim -21$ mag. However, the nature of SN 2011kl is still in debate. Greiner et al. (2015) suggest that it is an SN while Ioka et al. (2016) argue that it might be a TDE. If SN 2011kl is a TDE, the peak bolometric magnitude of most luminous GRB-SN is $\gtrsim -19$ mag.

Matsumoto et al. (2016) investigated the model supposing that the jet successfully breaks out and generates a GRB while the forward shock and the reverse shock produced will shock the envelope material and form a hot cocoon. Matsumoto et al. (2016) calculated the cocoon emission associated with the black hole-disk system produced by supermassive population III stars whose masses are $\sim 10^5 M_\odot$ at high redshift ($z \gtrsim 6$) and found that the jet cocoons will significantly enhance the optical luminosities of the SNe associated with the GRBs and predicted that the jet-cocoon emission will power very luminous SNe whose peak luminosities are $\sim 10^{45-46}$ erg s⁻¹ (the corresponding peak bolometric magnitudes are $\simeq -24$ mag to $\simeq -26$ mag) after the cocoon breakout of the envelopes. While these high-redshift, superluminous GRB-SLSNe have not yet been discovered, Matsumoto et al. (2016) expect that they will be detected by upcoming NIR telescopes.

⁴ For example, the SFR of the host galaxy of PS1-10bjz is $2 - 3 M_\odot \text{ yr}^{-1}$. Since the mass of this host galaxy is $\approx 2.4 \times 10^7 M_\odot$, its specific SFR (sSFR) is $\approx 10^{-7} \text{ yr}^{-1} = 10^2 \text{ Gyr}^{-1}$ (Lunnan et al., 2013). Using the high angular-resolution UV imaging obtained by HST, Lunnan et al. (2015) studied the morphological properties, sizes, and SFR densities of the host galaxies of 16 SLSNe I and found that these galaxies are compact, irregular galaxies and their UV-derived SFR densities are high (the averaged value is $\simeq 0.1 M_\odot \text{ yr}^{-1} \text{ kpc}^{-2}$, Lunnan et al. 2015).

⁵ For example, the metallicity of the host galaxies of SN 2007bi, PS1-10bjz and SN 2010gx are $1/3 Z_\odot$ (Young et al., 2010), $0.1 Z_\odot$ (Lunnan et al., 2013) and $0.06 Z_\odot$ (Chen et al., 2013), respectively.

5.5 SLSNe vs. tidal disruption events (TDEs)

Judging whether a superluminous optical transient is a SLSN is rather challenging. As pointed out by Quimby et al. (2013a), it is very difficult to distinguish among the active galactic nuclei (AGN), tidal disruption events (TDEs) and SLSNe even if we have multi-band photometry, spectra and high resolution images.

For example, Vinko et al. (2015) demonstrated that the very luminous ($L_{\text{peak}} > 5 \times 10^{44} \text{ erg s}^{-1}$) optical transient *Dougie* might be a super-Eddington TDE, rather than a SLSN; Dong et al. (2016) suggested that ASASSN-15lh is the most luminous SN discovered so far while Leloudas et al. (2016) argued that it is a TDE.

Although modeling these luminous optical transients would help to determine their nature, comprehensive observations for their multi-band LCs and multi-epoch spectra are also needed.

6 CONCLUSIONS

In the past two decades, SLSNe whose peak luminosities are $\gtrsim 7 \times 10^{43} \text{ erg s}^{-1}$ have been discovered by many sky-survey telescopes and the efforts to unveil the energy sources and nature of SLSNe have been done by many groups. The LCs and spectra of SLSNe are rather heterogeneous, reflecting the diverse physical parameters, e.g., energies, ejecta masses, ejecta velocities, and some other parameters associated with their central remnants which might play key roles in powering their LCs. Observing SLSNe and modeling their LCs offer new opportunities to study the evolution and explosion mechanisms of massive stars.

In this *review*, we present five single energy-source models which have been used to explain the LCs of SLSNe (and normal SNe), i.e., the ^{56}Ni cascade decay model, the magnetar model, the ejecta-CSM interaction model, the fallback (jet-ejecta interaction) model, the cooling model, as well as their different combinations.

Unlike normal SNe whose LCs can be reasonably explained by the models mentioned above, it is much less clear how SLSNe can be powered by these plausible energy sources. The LCs of normal SNe are mainly powered by ^{56}Ni cascade decay and the role of neutron-star spinning-down and the ejecta-CSM interaction can be neglected in the modeling for most SNe, except for types IIn, Ibn and Ia-CSM SNe. On the other hand, accumulating observational data and theoretical modeling indicate that the ^{56}Ni model cannot account for most of the LCs of SLSNe and luminous SNe since this scenario requires a huge amount of ^{56}Ni inside the ejecta to account for their peak luminosities and that the energy from nascent magnetars or ejecta-CSM interaction can play an essential role in powering the LCs of a majority of SLSNe and luminous SNe. But we cannot conclude that these SLSNe must be powered by magnetars or ejecta-CSM interaction and cannot discriminate between these two models even if the LCs of SLSNe can be explained by one of or both these two models. To account for the complicated LCs of some SLSNe, the triple-energy-source model might be employed.

The cooling emission from shock-heated envelopes of the progenitors would produce the first peaks of the LCs of some SLSNe having double-peaked LCs and the emission from ^{56}Ni or magnetar or ejecta-CSM interactions can power the second peaks. The first peaks might usually be missed due to the lack of very early observations for some SLSNe.

An appealing unified scenario is that type I SLSNe, type IIL SLSNe, luminous SNe Ic and normal SNe Ic are powered by neutron stars plus ^{56}Ni while type IIn SLSNe, luminous SNe IIn and normal SNe IIn are powered by the ejecta-CSM interaction plus ^{56}Ni . In this scenario, the ^{56}Ni masses are roughly constant ($\sim 0.1M_{\odot}$), the difference of the neutron-star properties (the initial rotational periods P_0 , the magnetic field strength B) or the ejecta and CSM properties (the ejecta mass, the ejecta velocity, the CSM mass, the CSM density profile, and so on) result in different luminosity and rise/decline rate, while the ejecta masses and velocities determine the LC width.

Extreme conditions are required if these models are valid for explaining SLSNe. For SLSNe powered by ^{56}Ni , a huge amount ($\gtrsim 5M_{\odot}$) of ^{56}Ni must be synthesized and the SNe might be PISNe; For SLSNe powered by magnetars, magnetars with very short initial rotational periods ($P_0 \lesssim 10 \text{ ms}$)

and very strong magnetic field strength ($\gtrsim 10^{13-15}$ G) must be left after explosions and the SNe must be CCSNe; For SLSNe powered by ejecta-CSM interactions or shell-shell interactions, the progenitors might be η Carinae-like stars and must experience strong wind loss or (multiple) giant eruptions (just) prior to the explosions and the final explosions can be CCSNe or PISNe, depending on the ^{56}Ni masses required.

Although the most prevailing semi-analytic models can yield LCs that are in good agreement with the photometric observations, their disadvantages are obvious: neglecting the time- and space-dependent effect of optical opacity, the mixing effect, and the two/three-dimensional effect. Besides, some very luminous optical transients having very bright peak luminosities (peak absolute magnitudes are $\lesssim -20.5$ mag) and very short rising time scales ($\lesssim 10$ days) cannot be well explained by any models mentioned above. More detailed modeling might provide more useful information and eventually determine their nature and their energy sources.

Determining the energy sources of SLSNe requires more dedicated observations and theoretical studies. Radio and X-ray observations for the remnants of some SLSNe also help us to judge whether or not the LCs of SLSNe are powered by magnetars or the ejecta-CSM interactions or other complicated models. New sky-survey programs (the Zwicky Transient Facility (ZTF), Law et al. 2009) and the upcoming sky-survey programs (e.g., the Large Synoptic Survey Telescope (LSST), Ivezić et al. 2008; LSST Science Collaborations et al. 2009), would discover more nearby SLSNe and intense follow-up photometric and spectral observations for them would shed more light on the nature of these optical transients. Modeling these SLSNe would help to determine their energy sources.

Acknowledgements We thank Weikang Zheng for helpful discussions. This work was supported by the National Key Research and Development Program of China (grant No. 2017YFA0402600) and the National Natural Science Foundation of China (grant No. 11573014 and 11833003).

References

- Agnolletto, I., Benetti, S., Cappellaro, E., et al. ApJ, 2009, 691, 1348
 Arcavi, I., Wolf, W. M., Howell, D. A., et al. 2016, ApJ, 819, 35
 Arnett, W. D. 1982, ApJ, 253, 785
 Ashall, C., Pian, E., Mazzali, P. A., et al. 2017, arXiv:1702.04339
 Baade, W., & Zwicky, F. 1934, Phys. Rev, 46, 76
 Barkat, Z., Rakavy, G., & Sack, N. 1967, Phys. Rev. Lett., 18, 379
 Berger, E., Chornock, R., Holmes, T. R., et al. 2011, ApJ, 743, 204
 Bersten, M. C., Benvenuto, O. G., Orellana, M., & Nomoto, K. 2016, ApJL, 817, L8
 Blanchard, P. K., Nicholl, M., Berger, E., et al. 2018, arXiv:1810.11051
 Bose, S., Dong, S., Pastorello, A., et al. 2018, ApJ, 853, 57
 Bucciantini, N., Quataert, E., Arons, J., Metzger, B. D., & Thompson, T. A. 2008, MNRAS, 383, L25
 Campana, S., Mangano, V., Blustin, A. J., et al. 2006, Nature, 442, 1008
 Cano, Z., de Ugarte Postigo, A., Perley, D. et al. MNRAS, 2015, 452, 1535
 Cano, Z., de Ugarte Postigo, A., Pozanenko, A. et al. 2014, A&A, 568, A19
 Cano, Z., Izzo, L., de Ugarte Postigo, A., et al. 2017a, A&A, 605, A107
 Cano, Z., Wang, S. Q., Dai, Z. G., Wu, X. F. 2017b, Advances in Astronomy, 8929054, 1
 Cappellaro, E., Mazzali, P. A., Benetti, S., et al. 1997, A&A, 328, 203
 Chatzopoulos, E., & Wheeler, J. C. 2012, ApJ, 760, 154
 Chatzopoulos, E., Wheeler, J. C., & Vinko, J. 2012, ApJ, 746, 121
 Chatzopoulos, E., Wheeler, J. C., & Sean M. C. 2013a, ApJ, 776, 129
 Chatzopoulos, E., Wheeler, J. C., Vinko, J., Horvath, Z. L., & Nagy, A. 2013b, ApJ, 773, 76
 Chen, K.-J., Moriya, T. J., Woosley, S., Sukhbold, T., Whalen, D. J., Suwa, Y., & Bromm, V. 2017, ApJ, 839, 85
 Chen, K.-J., Woosley, S. E., & Sukhbold, T. 2016, ApJ, 832, 73
 Chen, T.-W., Inserra, C., Fraser, M. et al. 2018, ApJL, 867, L31

- Chen, T.-W., Smartt, S. J., Bresolin, F., et al. 2013, *ApJL*, 763, L28
- Chen, T.-W., Smartt, S. J., Jerkstrand, A., et al. 2015, *MNRAS*, 452, 1567
- Chevalier, R. A. 1982, *ApJ*, 258, 790
- Chevalier, R. A., & Fransson, C. 1994, *ApJ*, 420, 268
- Chevalier, R. A., & Irwin, C. M. 2011, *ApJL*, 729, L6
- Chugai, N. N. 2009, *MNRAS*, 400, 866
- Chugai, N. N., & Danziger, I. J. 1994, *MNRAS*, 268, 173
- Chomiuk, L., Chornock, R., Soderberg, A. M., et al. 2011, *ApJ*, 743, 114
- Colgate, S. A., & McKee, C. 1969, *ApJ*, 157, 623
- Colgate, S. A., Petschek, A. G., & Kriese, J. T. 1980, *ApJL*, 237, L81
- Cooke, J., Sullivan, M., Gal-Yam, A., et al. 2012, *Nature*, 491, 228
- D'Elia, V., Pian, E., Melandri, A. et al. 2015, *A&A*, 577, 116
- Dai, Z. G., & Lu, T. 1998a, *A&A*, 333, L87
- Dai, Z. G., & Lu, T. 1998b, *PhRvL*, 81, 4301
- Dai, Z. G. 2004, *ApJ*, 606, 1000
- Dai, Z. G., & Liu, R. Y. 2012, *ApJ*, 759, 58
- Dai, Z. G., Wang, S. Q., Wang, J. S., Wang, L. J., & Yu, Y. W. 2016, *ApJ*, 817, 132
- De Cia, A., Gal-Yam, A., Rubin, A., et al. 2018, *ApJ*, 860, 100
- Dessart, L., & Hillier, D. J. 2005, *A&A*, 437, 667
- Dessart, L., Hillier, D. J., Waldman, R., Livne, E., & Blondin, S. 2012, *MNRAS*, 426, L76
- Deustua, S., Goldhaber, G., Groom, D., et al. 1995, *IAUC*, 6270
- Dexter, J., & Kasen, D. 2013, *ApJ*, 772, 30
- Dong, S. B., Shappee, B. J., Prieto, J. L., et al. 2016, *Science*, 351, 257
- Filippenko, A. V. 1997, *ARA&A*, 35, 309
- Galama, T. J., Vreeswijk, P. M., van Paradijs, J., et al. 1998, *Nature*, 395, 670
- Gal-Yam, A. 2012, *Science*, 337, 927
- Gal-Yam, A. 2018, *ARA&A*, arXiv:1812.01428
- Gal-Yam, A., Mazzali, P., Ofek, E. O., et al. 2009, *Nature*, 462, 624
- Gal-Yam, A., Moon, D. S., Fox, D. B., et al. 2004, *ApJL*, 609, L59
- Gao, H., Lei, W. H., You, Z. Q., & Xie, W. 2016, *ApJ*, 826, 141
- Gezari, S., Halpern, J. P., Grupe, D., et al. 2009, *ApJ*, 690, 1313
- Ginzburg, S., & Balberg, S. 2012, *ApJ*, 757, 178
- Greiner, J., Mazzali, P. A., Kann, D. A., et al. 2015, *Nature*, 523, 189
- Heger, A., & Woosley, S. E. 2002, *ApJ*, 567, 532
- Heger, A., Fryer, C. L., Woosley, S. E., et al. 2003, *ApJ*, 591, 288
- Hjorth, J., & Bloom, J. S. 2012, in Chapter 9 in *Gamma-Ray Bursts*, ed. C. Kouveliotou, R. A. M. J. Wijers, & S. Woosley (Cambridge Astrophysics Series, Vol. 51; Cambridge: Cambridge Univ. Press), 169
- Hjorth, J., Sollerman, J., Møller, P., et al. 2003, *Nature*, 423, 847
- Howell, D. A., Sullivan, M., Nugent, P. E., et al. 2006, *Nature*, 443, 308
- Inserra, C., Nicholl, M., Chen T.-W., et al. 2017, *MNRAS*, 468, 4642
- Inserra, C., Smartt, S. J., Jerkstrand, A., et al. 2013, *ApJ*, 770, 128
- Inserra, C., Smartt, S. J., Gall, E. E. E., et al. 2018, *MNRAS*, 475, 1046
- Ioka, K., Hotokezaka, K., & Piran, T. 2016, *ApJ*, 833, 110
- Ivezic, Z., Tyson, J. A., Abel, B., et al. 2008, arXiv:0805.2366
- Janka, H.-T. 2012, *Annual Review of Nuclear and Particle Science*, 62, 1, 407
- Janka, H.-T., Langanke, K., Marek, A., Martinez-Pinedo, G., & Müller, B. 2007, *Physics Reports*, 442, 1-6, 38
- Kasen, D., & Bildsten, L. 2010, *ApJ*, 717, 245
- Kasen, Daniel, & Woosley, S. E. 2009, *ApJ*, 703, 2205
- Kangas, T., Blagorodnova, N., Mattila, S., et al. 2017, *MNRAS*, 469, 1246
- Kann, D. A., Schady, P., Olivares E., F., et al. 2016, arXiv:1606.06791

- Kotera, K., Phinney, E. S., & Olinto, A. V. 2013, *MNRAS*, 432, 3228
- Kozyreva, A., & Blinnikov, S. 2015, *MNRAS*, 454, 4357
- Law, N. M., Kulkarni, S. R., Dekany, R. G., et al. 2009, *PASP*, 121, 1395
- Leloudas, G., Chatzopoulos, E., Dilday, B., et al. 2012, *A&A*, 541, 129
- Leloudas, G., Fraser, M., Stone, N. C., et al. 2016, *NatAs*, 1, 2
- Liu, L. D., Wang, L. J., Wang, S. Q., & Dai, Z. G. 2018, *ApJ*, 856, 59
- Liu, L. D., Wang, S. Q., Wang, L. J., Dai, Z. G., Yu, H., & Peng, Z. K. 2017, *ApJ*, 842, 26
- Liu, Y.-Q., & Modjaz, M. 2017, *ApJ*, 845, 85
- LSST Science Collaborations et al., 2009, arXiv:0912.0201
- Lundqvist, P., Kozma, C., Sollerman, J., et al. 2001, *A&A*, 374, 629
- Lunnan, R., Chornock, R., Berger, E., et al. 2013, *ApJ*, 771, 97
- Lunnan, R., Chornock, R., Berger, E., et al. 2014, *ApJ*, 787, 138
- Lunnan, R., Chornock, R., Berger, E., et al. 2015, *ApJ*, 804, 90
- Lunnan, R., Chornock, R., Berger, E., et al. 2018, *ApJ*, 852, 81
- MacFadyen, A. I., & Woosley, S. E. 1999, *ApJ*, 524, 262
- Maeda, K., Tanaka, M., Nomoto, K., et al. 2007, *ApJ*, 666, 1069
- Matsumoto, T., Nakauchi, D., Ioka, K., & Nakamura, T. 2016, *ApJ*, 823, 83
- Mazzali, P. A., Deng, J., Nomoto, K., et al. 2006, *Nature*, 442, 1018
- McCrum, M., Smartt, S. J., Rest, A., et al. 2015, *MNRAS*, 448, 1206
- Melandri, A., Pian, E., Ferrero, P., et al. 2012, *A&A*, 547, 82
- Metzger, B. D., Giannios, D., Thompson, T. A., Bucciantini, N., & Quataert, E. 2011, *MNRAS*, 413, 2031
- Metzger, B. D., Margalit, B., Kasen, D., & Quataert, E. 2015, *MNRAS*, 454, 3311
- Metzger, B. D., Thompson, T. A., & Quataert, E. 2007, *ApJ*, 659, 561
- Minkowski, R. 1941. *PASP*, 53, 22
- Miller, A. A., Chornock, R., Perley, D. A., et al. 2009, *ApJ*, 690, 1303
- Miller, A. A., Silverman, J. M., Butler, N. R., et al. 2010, *MNRAS*, 404, 305
- Moriya, T. J., Blinnikov, S. I., Tominaga, N., Yoshida, N., Tanaka, M., Maeda, K., & Nomoto, K. 2013, *MNRAS*, 428, 1020
- Moriya, T. J., Chen, T.-W., & Lange, N. 2017, *ApJ*, 835, 177
- Moriya, T. J., Nicholl, M., & Guillochon, J. *ApJ*, 867, 113
- Neill, J. D., Sullivan, M., Gal-Yam, A., et al. 2011, *ApJ*, 727, 15
- Nicholl, M., Berger, E., Smartt, S. J., et al. 2016a, *ApJ*, 826, 39
- Nicholl, M., Berger, E., Margutti, R., et al. 2016b, *ApJL*, 828, L18
- Nicholl, M., Berger, E., Margutti, R., Blanchard, P. K., Milisavljevic, D., Challis, P., Metzger, B. D., & Chornock, R. 2017a, *ApJL*, 835, L8
- Nicholl, M., Berger, E., Margutti, R., Blanchard, P. K., Guillochon, J., Leja, J., & Chornock, R. 2017b, *ApJL*, 845, L8
- Nicholl, M., Blanchard, P. K., Berger, E., et al. 2018, *ApJL*, 866, L24
- Nicholl, M., Jerkstrand, A., Inserra, C., et al. 2014, *MNRAS*, 444, 2096
- Nicholl, M., Smartt, S. J., Jerkstrand, A., et al. 2013, *Nature*, 502, 346
- Nicholl, M., Smartt, S. J., Jerkstrand, A., et al. 2015a, *ApJL*, 807, L18
- Nicholl, M. & Smartt, S. J. 2016, *MNRAS*, 457, L79
- Ostriker, J. P., & Gunn, J. E. 1971, *ApJL*, 164, L95
- Pastorello, A., Mattila, S., Zampieri, L., et al. 2008, *MNRAS*, 389, 113
- Pastorello, A., Smartt, S. J., Botticella, M. T., et al. 2010, *ApJL*, 724, L16
- Piro, A. L. 2015, *ApJL*, 808, L51
- Piro, A. L. & Nakar, E. 2013, *ApJ*, 769, 67
- Popov, D. V. 1993, *ApJ*, 414, 712
- Quimby, R. M. 2014, *IAUS*, 296, 68
- Quimby, R. M., Kulkarni, S. R., Kasliwal, M. M., et al. 2011, *Nature*, 474, 487
- Quimby, R. M., Yuan, F., Akerlof, C., et al. 2013a, *MNRAS*, 431, 912

- Rakavy, G., & Shaviv, G. 1967, *ApJ*, 148, 803
- Roy, R., Sollerman, J., Silverman, J. M., et al. 2016, *A&A*, 596, 67
- Sanders, N. E., Soderberg, A. M., Valenti, S., et al. 2012, *ApJ*, 756, 184
- Schlegel, E. M. 1990, *MNRAS*, 244, 269
- Schlegel, E. M. 1996, *AJ*, 111, 1660
- Schmidt, B., Tonry, J., Barris, B., et al. 2000, *IAUC.*, 7516, 1
- Smartt, S. J. 2009, *ARA&A*, 47, 63
- Smith, N., Li, W., Foley, R. J., et al. 2007, *ApJ*, 666, 1116
- Smith, N., & McCray, R. 2007, *ApJL*, 671, L17
- Smith, M., Sullivan, M., D'Andrea, C. B., et al. 2016, *ApJL*, 818, L8
- Smith, N. 2016, arXiv:1612.02006
- Soker, N., & Gilkis, A. 2017, *ApJ*, 851, 95
- Sollerman, J., Holland, S. T., Challis, P., et al. *A&A*, 386, 944
- Stanek, K. Z., Matheson, T., Garnavich, P. M., et al. 2003, *ApJL*, 591, L17
- Starling, R. L. C., Wiersema, K., Levan, A. J., et al. 2011, *MNRAS*, 411, 2792
- Sukhbold, T., Ertl, T., Woosley, S. E., Brown, J. M., & Janka, H.-T. 2016, *ApJ*, 821, 38
- Taddia, F., Sollerman, J., Leloudas, G., et al. 2015, *A&A*, 574, 60
- Tolstov, A., Nomoto, K., Blinnikov, S., Sorokina, E., Quimby, R., & Baklanov, P. 2017, *ApJ*, 835, 266
- Toy, V. L., Cenko, S. B., Silverman, J. M., et al. 2016, *ApJ*, 818, 79
- Ugliko, M., Janka, H.-T., Marek, A., et al. 2012, *ApJ*, 757, 69
- Umeda, H., & Nomoto, K. 2008, *ApJ*, 673, 1014
- Usov, V. V. 1992, *Natur*, 357, 472
- Valenti, S., Benetti, S., Cappellaro, E., et al. 2008, *MNRAS*, 383, 1485
- Vinko, J., Quimby, R. M., Wheeler, J. C., Ramirez-Ruiz, E., Guillochon, J., Chatzopoulos, E., Marion, G. H., & Akerlof, C. 2015, *ApJ*, 798, 12
- Vreeswijk, P. M., Leloudas, G., Gal-Yam, A., et al. 2017, *ApJ*, 835, 58
- Wang, L. J., Cano, Z., Wang, S. Q., et al. 2017a, *ApJ*, 851, 54
- Wang, L. J., Han, Y. H., Xu, D., et al. 2016a, *ApJ*, 831, 41
- Wang, L. J., Wang, S. Q., Dai, Z. G., Xu, D., Han, Y. H., Wu, X. F., & Wei, J. Y. 2016b, *ApJ*, 821, 22
- Wang, L. J., Wang, X. F., Cano, Z., et al. 2017b, submitted (arXiv:1712.07359)
- Wang, L. J., Wang, X. F., Wang, S. Q., et al. 2018, *ApJ*, 865, 95
- Wang, L. J., Yu, H., Liu, L. D., Wang, S. Q., Han, Y. H., Xu, D., Dai, Z. G., Qiu, Y. L., & Wei, J. Y. 2017c, *ApJ*, 837, 128
- Wang, S. Q., Cano, Z., Wang, L. J., et al. 2017d, *ApJ*, 850, 148
- Wang, S. Q., Liu, L. D., Dai, Z. G., Wang, L. J., & Wu, X. F. 2016c, *ApJ*, 828, 87
- Wang, S. Q., Wang, L. J., Dai, Z. G., & Wu, X. F. 2015a, *ApJ*, 799, 107
- Wang, S. Q., Wang, L. J., Dai, Z. G., & Wu, X. F. 2015b, *ApJ*, 807, 147
- Waxman, E., & Katz, B. 2016, arXiv:1607.01293
- Woosley, S. E. 1993, *ApJ*, 405, 273
- Woosley, S. E. 2010, *ApJL*, 719, L204
- Woosley, S. E., Blinnikov, S., & Heger, A. 2007, *Nature*, 450, 390
- Woosley, S. E., & Bloom, J. S. 2006, *ARA&A*, 44, 507
- Xu, D., de Ugarte Postigo, A., Leloudas, G., et al. 2013, *ApJ*, 776, 98
- Yan, L., Quimby, R., Gal-Yam, A., et al. 2017, *ApJ*, 840, 57
- Yan, L., Quimby, R., Ofek, E., et al. 2015, *ApJ*, 814, 108
- Young, D. R., Smartt, S. J., Valenti, S., et al. 2010, *A&A*, 512, A70
- Zhang, B., & Mészáros, P. 2001, *ApJL*, 552, L35
- Zhang, T. M., Wang, X. F., Wu, C., et al. 2012, *AJ*, 144, 131